



OPEN ACCESS

EDITED BY

Marie Antonette Juinio-Meñez,
University of the Philippines Diliman,
Philippines

REVIEWED BY

Francisco Solís,
Institute of Marine Science and
Limnology, National Autonomous
University of Mexico, Mexico
Owen Anderson,
National Institute of Water and
Atmospheric Research (NIWA), New
Zealand

*CORRESPONDENCE

Ning Xiao
xiaoning@qdio.ac.cn

[†]These authors have contributed
equally to this work and share
first authorship

SPECIALTY SECTION

This article was submitted to
Marine Biology,
a section of the journal
Frontiers in Marine Science

RECEIVED 05 September 2022

ACCEPTED 21 October 2022

PUBLISHED 09 December 2022

CITATION

Zheng W, Sun S, Sha Z and Xiao N
(2022) Three new species and two
new records of Echinothuriidae
(Echinodermata: Echinothurioida)
from seamounts in the Northwest
Pacific Ocean: Diversity,
phylogeny and biogeography of
deep-sea echinothuriids.
Front. Mar. Sci. 9:1036914.
doi: 10.3389/fmars.2022.1036914

COPYRIGHT

© 2022 Zheng, Sun, Sha and Xiao. This
is an open-access article distributed
under the terms of the [Creative
Commons Attribution License \(CC BY\)](#).
The use, distribution or reproduction
in other forums is permitted, provided
the original author(s) and the
copyright owner(s) are credited and
that the original publication in this
journal is cited, in accordance with
accepted academic practice. No use,
distribution or reproduction is
permitted which does not comply with
these terms.

Three new species and two new records of Echinothuriidae (Echinodermata: Echinothurioida) from seamounts in the Northwest Pacific Ocean: Diversity, phylogeny and biogeography of deep-sea echinothuriids

Wanrui Zheng^{1†}, Shao'e Sun^{1,2,3,4†}, Zhongli Sha^{1,2,3,4}
and Ning Xiao^{1,2,3,4*}

¹Department of Marine Organism Taxonomy and Phylogeny, Institute of Oceanology, Chinese Academy of Sciences, Qingdao, China, ²Laboratory for Marine Biology and Biotechnology, Qingdao National Laboratory for Marine Science and Technology, Qingdao, China, ³Shandong Province Key Laboratory of Experimental Marine Biology, Institute of Oceanology, Chinese Academy of Sciences, Qingdao, China, ⁴College of Marine Science, University of Chinese Academy of Sciences, Beijing, China

The soft sea urchins Echinothuriidae Thomson, 1872, constitute the most commonly encountered sea urchins in the bathyal environment. The echinothuriids are common and frequently abundant in the Indo-Pacific, but the species diversity is still not completely known yet. Our examination of echinoid specimens collected from seven seamounts in the Northwest Pacific Ocean revealed three new species and two new records. The three new species are described as *Araeosoma cucullatum* sp. nov., *Araeosoma polyporum* sp. nov., and *Hygrosoma involucrum* sp. nov. The two new records included two species from the genus *Araeosoma*. They are distinguished from each other and from congeners by the following characteristics: coloring, ambulacrum, interambulacrum, apical system, spines, and pedicellariae. The identities of the five species are well supported by genetic distance and phylogenetic analyses based on the mitochondrial *cytochrome oxidase subunit I (COI)* and *16S rRNA* genes. Based on the distribution data, we explored the distribution patterns of *Araeosoma*, *Calveriosoma*, *Hapalosoma*, *Sperosoma*, *Tromikosoma*, and *Hygrosoma*, the six echinothuriid genera occurring in deep sea, and delineated 10 isolated deep-sea biogeographic provinces all over the world. The Western Pacific harbors higher species diversity of deep-sea echinothuriids than other sea areas worldwide, indicating that the Western Pacific may play an important part in the dispersal and speciation of deep-sea echinothuriids.

KEYWORDS

Echinothuriidae, new species, deep sea, biodiversity, biogeography, new records

Introduction

The order Echinothurioida Claus, 1880, includes the families Echinothuriidae Thomson, 1872a; Kamptosomatidae Mortensen, 1934; and Phormosomatidae Mortensen, 1934. As the largest family, Echinothuriidae includes 53 accepted species, which belong to seven genera (*Araeosoma* Mortensen, 1903; *Asthenosoma* Grube, 1868; *Calveriosoma* Mortensen, 1934; *Hapalosoma* Mortensen, 1903; *Hygrosoma* Mortensen, 1903; *Sperosoma* Koehler, 1897; and *Tromikosoma* Mortensen, 1903) (Kroh and Mooi, 2022). The distinctive hoof-like tip of the oral spines is the most characteristic feature of this family (Thomson, 1872a; Mortensen, 1935). The family Echinothuriidae is the most commonly encountered sea urchin in the deep ocean. They are primarily deep-sea inhabitants, with most species observed at bathyal depths. Only the members of the Indo-Pacific genus *Asthenosoma* Grube, 1868 are observed in shallow depths (Mortensen, 1927; David and Sibuet, 1985; Stevenson and Kroh, 2020).

Araeosoma is the largest genus in Echinothuriidae. Currently, 19 species are included in this genus. Dactylous pedicellariae is a special characteristic of this genus, with nothing similar being known to occur in any other echinothurid or in other echinoids (Mortensen, 1935). The genus *Hygrosoma* is characterized by having ambulacral pores on the oral surface arranged in a single series near the adradial margin, as well as oral primary spines with conspicuously large flaring hoofs (Anderson, 2016). This genus is currently composed of three species: *Hygrosoma hoplanchtha* (Thomson, 1877), *Hygrosoma luculentum* (Agassiz, 1879), and *Hygrosoma petersii* (Agassiz, 1880).

Mooi et al. (2004) studied the phylogenetic relationship of the echinothurioids and confirmed that they are monophyletic

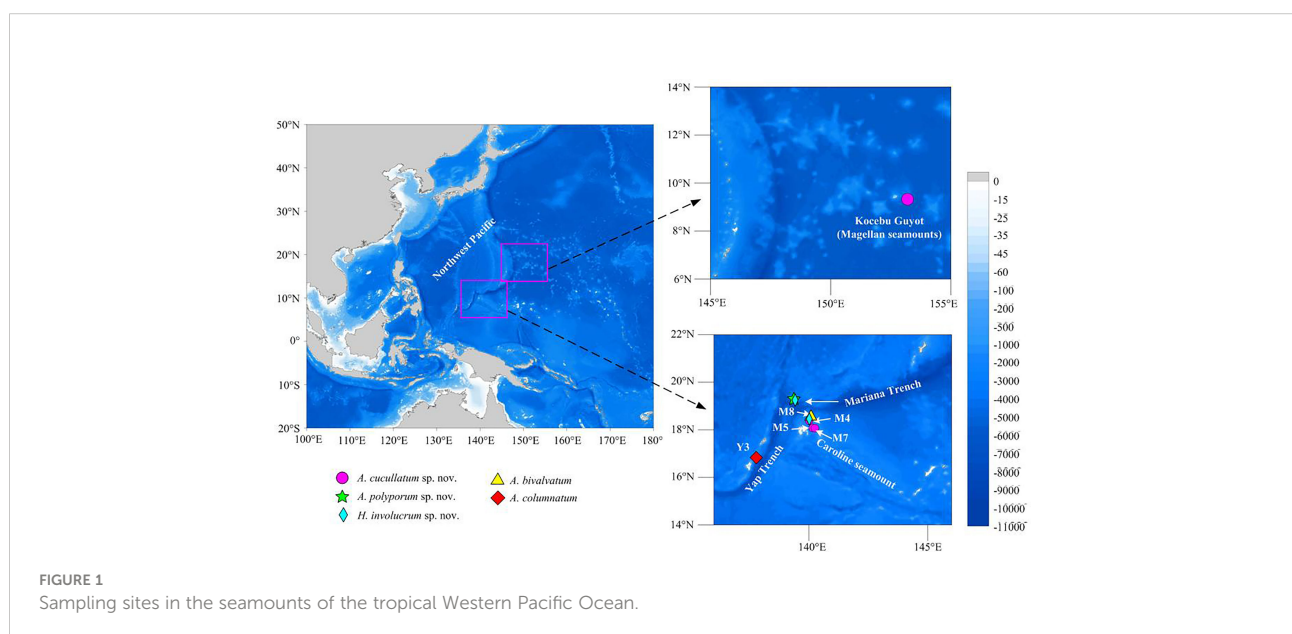
and basal to most other extant echinoid groups. Anderson (2013; 2016) examined a large collection of echinothurioid echinoids from museum collections in New Zealand and Australia and described eight species in the genus *Araeosoma* and one in the genus *Hygrosoma*. Thereafter, *Araeosoma* and *Hygrosoma* have seldom been reported or investigated in the world oceans.

During surveys of the benthos in the Northwest Pacific Ocean from 2014 to 2019, we collected 11 specimens of *Araeosoma* and seven specimens of *Hygrosoma* from seven seamounts. These new materials provide an opportunity to present: i) descriptions of three new species and two new records; ii) assessment of the intraspecific divergence between the new species and all other known species; iii) evaluation of the systematic status of Echinothuriidae; and iv) discussion of the diversity and distribution and the biogeography of deep-sea echinothuriids. Our study provides new insights into the diversity, phylogeny, and distribution of deep-sea echinothuriids.

Materials and methods

Sampling and preservation

Specimens were collected from the Magellan (Kocebu Guyot), Yap (Y3), Mariana, and Caroline (M4, M5, M7, and M8) seamount areas (207–1,605 m) (Figure 1) using the Remotely Operated Vehicle submersible (ROV) FaXian (Discovery) on board the R/V *KEXUE* (Science) from 2014 to 2019. Subsequently, the specimens were immediately preserved in 75% ethanol and deposited at the Marine Biological Museum of Chinese Academy of Sciences (MBMCAS), Institute of Oceanology, Chinese Academy of Sciences (IOCAS).



Morphology observation

The morphological characteristics of the outer test of Echinothuriidae urchins were observed under a stereomicroscope (ZEISS Stemi 2000-C, Wetzlar, Germany). Several pedicellariae of each type that could be found on the type specimens were removed using fine forceps. The pedicellariae were digested in 10% solution of sodium hypochlorite to separate and remove the soft tissue from the individual valves (Anderson, 2013). To avoid over exposure to hydrogen peroxide, which might damage the ossicles, this digestion process was observed under a stereomicroscope. The pedicellaria ossicles were then washed three times in distilled water and dried in absolute ethanol (Coppard and Schultz, 2006). The individual valves and whole pedicellariae were then examined with a scanning electron microscope (Hitachi S-3400N, Tokyo, Japan) and the images recorded in digital format.

DNA extraction and sequencing

One specimen each of *Araeosoma alternatum*, *Araeosoma polyporum* sp. nov., and *Araeosoma bidentatum*; four specimens of *Araeosoma cucullatum* sp. nov.; and seven specimens of *Hygrosoma involucrum* sp. nov. were collected for gene sequencing. Total genomic DNA was extracted from the muscle tissue (<30 mg) from the base of the primary spines of each specimen using the E.Z.N.A.[®] Tissue DNA Kit (Omega Bio-Tek, Norcross, GA, USA) following the manufacturer's instructions. The DNA was eluted in 50 µl of sterile distilled H₂O (RNase free) and stored at -20°C. Mitochondrial cytochrome oxidase subunit I (*COI*) (~650 bp) and 16S rRNA (*16S*) (~600 bp) genes were amplified by polymerase chain reaction (PCR), which was carried out in a reaction mix containing 1 µl of template DNA, 15 µl of Premix Taq[™] (Takara, Otsu, Shiga, Japan), 1 µl of positive and negative primers (10 mM), and 12 µl of sterile distilled H₂O to a total volume of 30 µl.

The primer sequences for each gene region are listed in Supplementary Table S1. The PCR conditions consisted of an initial denaturation at 94°C for 5 min, followed by 35 cycles of denaturation at 94°C for 30 s, annealing at 52°C for 30 s, extension at 72°C for 1 min, and a final extension at 72°C for 7 min. The PCR products were examined with 1.5% agarose gel electrophoresis and purified using the EZ-10 Spin Column DNA Gel Extraction Kit (Sangon Biotech, Shanghai, China) before sequencing. The purified PCR products were bidirectionally sequenced using an ABI PRISM 3730 (Applied Biosystems, Foster City, CA, USA) automatic DNA sequencer with the same primer sets used for PCR amplification.

Barcoding and phylogenetic analyses

The sequencing data were visualized and edited with the Seqman program from DNASTAR (<http://www.DNASTAR.com>). Manual examination was applied to ensure correct assembly. The assembled sequences were checked using BLAST searches (ncbi.nlm.nih.gov) to ensure that the sequences were not contaminated. The new sequences were then deposited in GenBank under the accession numbers listed in Supplementary Table S2.

Two sequencing datasets were analyzed. The first dataset contained the barcoding sequences of *COI* from all available Echinothuriidae urchins, downloaded from BOLD (<https://www.boldsystems.org/>) and NCBI (<https://www.ncbi.nlm.nih.gov/>) databases, which was used to examine species delimitation (Supplementary Table S2). To determine the systematic status of the new Echinothuriidae species, the second dataset contained concatenated sequences of the *COI* and *16S* fragments of 94 species from Echinoidea and three outgroups from Holothuroidea (Supplementary Table S2). The sequences of *16S* were aligned using MAFFT version 5 (Katoh et al., 2005) with default parameters. For the protein-coding gene *COI*, alignment was conducted with MEGA v.6 (Tamura et al., 2013) based on codon positions. The Kimura two-parameter (K2P) genetic distances of *COI* among the Echinothuriidae species were calculated with MEGA v.6. Neighbor-joining (NJ) analysis of the Echinothuriidae species was conducted using MEGA v.6 based on the K2P model. Branch supports were estimated by bootstrapping with 1,000 replicates.

Phylogenetic trees were inferred from the concatenated sequences using the maximum likelihood (ML) and Bayesian inference (BI) methods. The best-fit partitioning schemes and substitution models were selected using PartitionFinder 2.1.1 (Lanfear et al., 2017) (Supplementary Table S3). ML analysis was carried out using the best-fit partition schemes and models in the IQ-TREE web server (Trifinopoulos et al., 2016). The branch support was assessed with 5,000 ultrafast bootstrap replicates (Minh et al., 2013). BI analysis was conducted with MrBayes 3.1 software (Ronquist and Huelsenbeck, 2003) using partition models. The Markov chain Monte Carlo (MCMC) was run for 50,000,000 generations, with sampling every 1,000 generation to allow adequate time for convergence. The first 25% of the sampled trees were discarded as burn-in, with the remaining trees used to estimate the 50% majority rule consensus tree and the Bayesian posterior probabilities (PPs). At the end of the run, the average standard deviation of split frequencies decreased to 0.01. The effective sample size (ESS) values for all sampled parameters were checked using Tracer v1.7 (Rambaut et al., 2018) to make sure convergence was reached.

Biogeographic analysis

Existing distribution data of the echinothuriid species of *Araeosoma*, *Calveriosoma*, *Hapalosoma*, *Sperosoma*, *Tromikosoma*, and *Hygrosoma* were extracted (Supplementary Table S4) from the Ocean Biodiversity Information System (<https://obis.org/>). The distribution maps of these genera were illustrated with the software Surfer 16. A database of presence (coded 1) and absence (coded 0) for 44 echinothuriid species was established for 29 deep-sea regions (Supplementary Table S5). Statistical analyses were conducted using the software PRIMER v6 (Plymouth Marine Laboratory, Plymouth, UK). The deep-sea biogeographic provinces were delineated based on the unweighted pair group method with arithmetic mean (UPGMA) cluster analysis (Bray–Curtis distance) of all the echinothuriid species.

Results

Taxonomy

Order Echinothurioida Claus, 1880

Family Echinothuriidae Thomson, 1872a

Subfamily Hygrosomatinae Smith and Wright, 1990

Genus *Hygrosoma* Mortensen, 1903

Type species

Phormosoma petersii A. Agassiz, 1880, by original designation

Hygrosoma involucrum sp. nov.

Diagnosis

Adults of large size. Color of ethanol-preserved test and spines, dark brown; tube feet, black. Primary tubercles limited to the outer half of the oral side. Pore pairs of the aboral arranged into three to two series. The hoof of the primary oral spines is white and large (about 8 mm), widely flared. Adapical spines invested in a dark brown skin sheath. Large involute tridentate pedicellariae with long, narrow blades, tip un-serrated; small involute tridentate pedicellariae with short, narrow blades, tip finely serrated. Triphyllous pedicellariae of the usual form. Ophicephalous pedicellariae not found (Figures 2–4).

Holotype

MBM286941, M4 seamount, station FX-Dive 136 (10°28' N, 140°05' E), depth 1,469 m, 20 August 2017.

Paratypes

MBM286947, a seamount near the Mariana Trench, station FX-Dive 70 (11°16' N, 139°25' E), depth 1,372 m, March 27, 2016.

MBM286954, a seamount near the Mariana Trench, station FX-

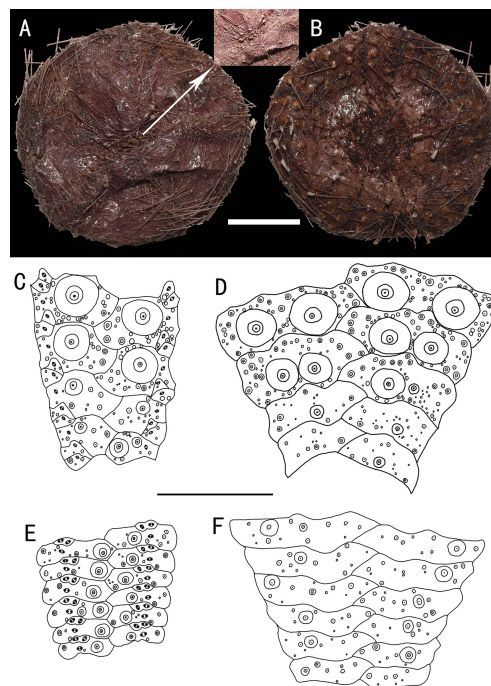


FIGURE 2

Hygrosoma involucrum sp. nov., holotype, MBM286941 (test diameter, 161 mm). (A) Aboral view. (B) Oral view. (C–F) Details of the coronal plates: (C), oral ambulacra (D), oral interambulacra (E), aboral ambulacra (F), aboral interambulacra. Scale bars, 50 mm (A, B) and 20 mm (C–F).

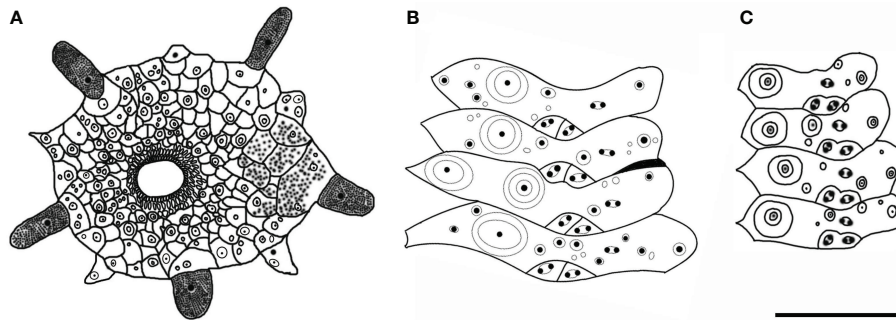


FIGURE 3

Hygrosoma involucrum sp. nov. (A) Paratype, MBM286940. Apical system. (B, C) Ambulacral plates from the aboral side: (B) from the paratype, MBM286970 (C) from the holotype, MBM286941. Scale bar, 10 mm.

Dive 62 (11°16' N, 139°22' E), depth 1,606 m, March 19, 2016. MBM286973, M4 seamount, station FX-Dive 137 (10°35' N, 140°07' E), depth 1,309 m, August 21, 2017. MBM286972, M4 seamount, station FX-Dive 137 (10°35' N, 140°07' E), depth 1,545 m, August 21, 2017. MBM286940, M4 seamount, station FX-Dive 136 (10°28' N, 140°05' E), depth 1,281 m, August 20, 2017. MBM286970, M4 seamount, station FX-Dive 138 (10°33' N, 140°07' E), depth 1,103 m, August 22, 2017.

Etymology

Named *involucrum*, from the Latin word *involucrum* (sheath), after spines near the apical system invested in a skin sheath.

Description

Test of holotype (Figures 2A, B): Approximately 161 mm test diameter (TD), flexible, flattened, and pentagonal in outline. Color

of ethanol-preserved test and spines, dark brown; tube feet, black. Ratio of ambulacrum to interambulacrum width at ambitus, 1:2.

There are 51–58 plates in each column of the interambulacral, with about 16–18 of these plates on the oral surface. There are 62–65 plates in each column of the ambulacral, with about 18–19 of these plates on the oral surface.

Oral test plating (Figures 2C, D): A primary tubercle occurs on every interambulacral plate from the ambitus to about half of the test, forming a regular adradial series. The other primary tubercles occur on every plate from the ambitus to about half of the test, forming a regular interradius series. In other specimens, e.g., MBM286973, primary tubercles also presented between these two series on a few of the plates. Numerous secondary and miliary tubercles are scattered over these plates. In the ambulacra, a primary tubercle occurs on every plate from the ambitus to about half of the test, forming a regular perradial series. Numerous secondary and miliary tubercles are scattered over these plates.

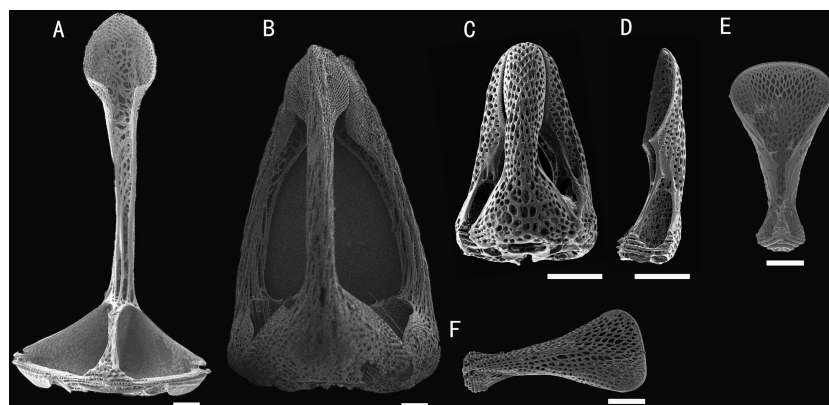


FIGURE 4

Hygrosoma involucrum sp. nov.; holotype, MBM286973. SEM images of pedicellariae. (A, B) Large involute tridentate pedicellaria: (A) individual valve (B) head. (C, D) Small involute tridentate pedicellaria: (C) head (D) individual valve. (E, F) Valves of triphyllous pedicellariae. Scale bar, 100 μ m.

The peristome is approximately 41 mm in diameter, with about four to five boomerang-shaped plates in each column. Each plate has a row of four to eight tubercles. The pore pairs are arranged in a single series. Peristomial spines and tube feet are dark brown colored. Gills moderate.

Aboral test plating (Figures 2E, F): Primary tubercles on the aboral side smaller than those of the oral side. A primary tubercle occurs on every interambulacral plate from the edge of the apical system to the ambitus, forming a regular adradial series. In other specimens, e.g., MBM286940, this differs in that the other primary tubercles occur on a few plates near to the ambitus, forming an irregular interradius series. In the ambulacra, a primary tubercle occurs on every plate, forming a regular perradial series. A few smaller primary tubercles parallel to those of the larger tubercles occur on a few plates. Numerous secondary and miliary tubercles are scattered over these plates. Pore pairs are arranged into two or three discrete columns in series (Figures 3B, C).

The apical system measures 24 mm in diameter, pentagonal. The genital pore is large, opening in the membranous gaps. What is more interesting is that, in one specimen observed, the genital plate is a long strip (Figure 3A). Madreporite distinct, slightly raised, split clearly into three to six sections. Ocular plate large, with one to three small tubercles.

Spines: Hollow and cylindrical, with the longest approximately 52 mm long, 1.5 mm in diameter. Primary spines of the oral surface are smooth, slightly curved, and with about 32 fine longitudinal striations. The hoof of the primary oral spines is white and large (about 8 mm), widely flared. Spines near the apical system invested in a dark brown skin sheath.

Pedicellariae (Figure 4): Two kinds of tridentate pedicellariae are present. One is a large involute form (head length about 1.4 mm) with long, narrow blades; the un-serrated tips about a third of the base width; and the blades in contact for only a small area. The other is an involute form (about 0.4 mm long) with short, narrow blades; the finely serrated tips about a third of the base width. The valves are in contact for nearly half of their length. Triphyllous pedicellariae (about 0.5–0.6 mm) the typical echinothurioid form.

Size range

The median TD of the seven specimens measured was 100 mm, with the largest specimen being 181 mm.

Distribution

Found on a seamount (M4) near the Caroline Ridge and a seamount near the Mariana Trench in the Northwest Pacific Ocean, where the water depth is about 1,103–1,606 m.

Remarks

The most obvious differences between *H. involucrum* sp. nov. and the other three known species of *Hygrosoma* are the characteristics of their pedicellariae. In *H. hoplacantha* (known from the Indo-Pacific), the large tridentate pedicellariae have a

broad, strongly involute blade with a distinctly serrated edge (see Figure 21 in Anderson, 2016). In *H. luculentum* (known from the Indo-Pacific), the short, broad-bladed with un-serrated edge tridentate pedicellariae usually present in great numbers (see Plate XIII, Figure 16 in Mortensen, 1903). None of these pedicellariae were found in the specimens examined.

The Atlantic *H. petersii* differs from the new species in terms of the absence of obvious membranous gaps in the apical system and adapical spines without skin sheath. In addition, the pore pairs of *H. petersii* are arranged into two close vertical series on the aboral side (Mortensen, 1935), while those of *H. involucrum* sp. nov. are arranged into two or three series.

Subfamily Echinothuriinae Thomson, 1872

Genus *Araeosoma* Mortensen, 1903

Type species

Calveria fenestrata Wyville Thomson, 1872, by original designation

Araeosoma cucullatum sp. nov.

Diagnosis

Adults of moderate size. The color of the ethanol-preserved test and spines is light brown, darker on the tissue surrounding the tubercles and tube feet, and the membranous gaps white. Membranous spaces widest in the median area between the plates of the interambulacra. A primary tubercle occurs on every interambulacral plate on the oral surface, forming a regular adradial series. The hoof of the primary oral spines is white, moderately long (about 1 mm), slightly flared, and slightly flattened distally. Three kinds of tridentate pedicellariae are present; large tridentate pedicellariae with spoon-shaped valves (Figures 5, 6).

Holotype

MBM286942, Kocebu Guyot, station FX-Dive 175 (17°20' N, 153°12' E), depth 1,314 m, April 9, 2018.

Paratypes

MBM286963, M4 seamount, station FX-Dive 132 (10°23' N, 140°09' E), depth 1,368 m, August 14, 2017. MBM286971, M7, station FX-Dive 223 (10°04' N, 140°15' E), depth 1,363 m, June 11, 2019. MBM286975, M5 seamount, station FX-Dive 214 (10°05' N, 140°10' E), depth 1,497 m, June 1, 2019.

Etymology

Named *cucullatum*, from the Latin word *cucullatus* (spoon-shaped), after the spoon-shaped valves of large tridentate pedicellariae.

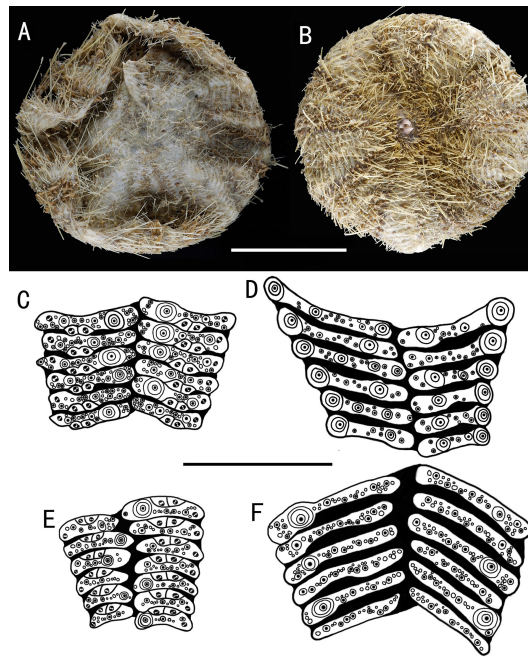


FIGURE 5

Araeosoma cucullatum sp. nov.; holotype, MBM286942 (test diameter, 105 mm). (A) Aboral view. (B) Oral view. (C–F) Details of the coronal plates: (C), oral ambulacra (D), oral interambulacra (E), aboral ambulacra (F) aboral interambulacra. Scale bars, 50 mm (A, B) and 20 mm (C–F).

Description

Test of holotype (Figures 5A, B): Approximately 105 mm TD, flexible, flattened, and circular in outline. The color of the ethanol-preserved test and spines is light brown, darker on the tissue surrounding the tubercles and tube feet, and the membranous

gaps white. Ratio of ambulacrum to interambulacrum width at ambitus, 3:4.

There are 34–41 plates in each column of the interambulacra, with about 17–19 of these plates on the oral surface. There are 43–51 plates in each column of the ambulacra, with about 21–25 of

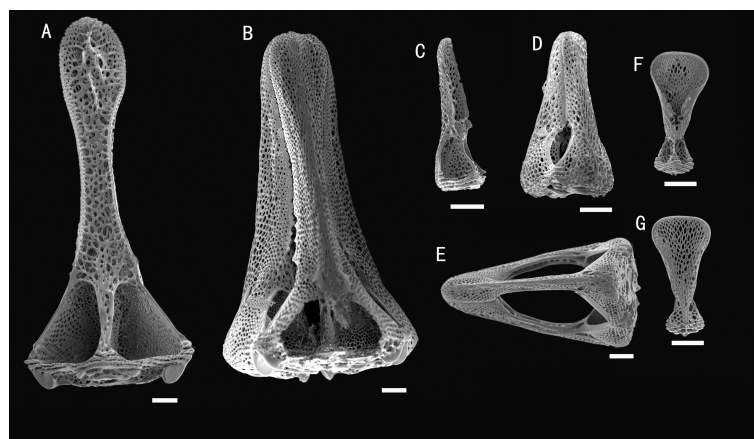


FIGURE 6

Araeosoma cucullatum sp. nov.; holotype, MBM286942. SEM images of pedicellariae. (A, B) Large tridentate pedicellaria: (A) individual valve (B) head. (C, D) Rostrate tridentate pedicellaria: (C) individual valve (D) head. (E) Involute tridentate pedicellaria. (F, G) Valves of triphyllous pedicellariae. Scale bar, 100 μ m.

these plates on the oral surface. Membranous spaces widest in the median area between interambulacral plates on the aboral surface. Adapical-most interambulacral plates angled slightly.

Oral test plating (Figures 5C, D): A primary tubercle occurs on every interambulacral plate from the edge of the peristome to the ambitus, forming a regular adradial series. The other primary tubercles occur on every plate or every second plate from the ambitus to about two-thirds of the test. These tubercles form an irregular series adjacent to the interradius. One or two secondary tubercles occur on a few plates. Numerous miliary tubercles scattered over on interambulacral plates. In the ambulacra, a primary tubercle occurs on every plate or every second plate, forming an irregular perradial series. Secondary tubercles are arranged irregularly on the adradial side and perradial side of the pore pairs. Numerous miliary tubercles are scattered over on ambulacra plates.

The peristome is approximately 23 mm in diameter, with about 10 boomerang-shaped plates in each column. Each plate has a row of two to three tubercles. The pore pairs are arranged in a single series. Peristomial spines and tube feet brown colored, the same color as that in the test. Gills large.

Aboral test plating (Figures 5E, F): A primary tubercle occurs on every second interambulacral plate from the ambitus to about four-fifths of the test, forming a regular adradial series. Numerous miliary tubercles scattered over these plates. In the ambulacra, a primary tubercle occurs between every plate to the fifth plate, forming an irregular perradial series. Numerous miliary tubercles are scattered over these plates.

The apical system measures 21 mm in diameter, pentagonal. Genital pores large, opening in the membranous gaps within the disaggregated genital plates. Madreporite distinct, slightly raised, kidney-shaped, and split clearly into one to two sections. Ocular plate large, with three to five small tubercles.

Spines: Hollow and cylindrical, with the longest approximately 14 mm long, 0.5 mm in diameter. The primary spines of the oral surface are smooth, slightly curved, and with about 20 fine, longitudinal striations. The hoof of the primary oral spines is white, moderately long (about 1.8 mm), slightly flared, and slightly flattened distally.

Pedicellariae (Figure 6): Three kinds of tridentate pedicellariae are present. A large kind (head length about 1.5 mm) with distinctly spoon-shaped valves, narrowest in the middle and widened distally, un-serrated tip. The valves are in contact for most of their length, and a base about two times the width of the tip. Two smaller types are also present: one rostrate form (about 0.4–0.6 mm long) with straight-sided, narrow, and un-serrated blades with a rounded tip; the other an involute form (about 1–1.5 mm long) with narrow, un-serrated blade, tips about one-fifth the valve length, and base about four times the width of the tip. Triphyllous pedicellariae (about 0.3–0.4 mm) of the typical echinothurioid form. Dactyloous pedicellariae not found.

Size range

The median TD of the four specimens measured was 98.5 mm, with the largest specimen being 118 mm.

Distributions

Found on a seamount (Kocebu Guyot) near the Magellan seamount and three seamounts (M4, M7, and M5) near the Caroline Ridge in the Northwest Pacific Ocean, where the water depth is about 1,314–1,497 m.

Remarks

The new species mostly resembles *Araeosoma coriaceum* (Agassiz, 1879) (known from the Indo-Pacific) in terms of test plate morphology and tuberculation. However, the two species differ in aspects of their tridentate pedicellariae, hoof of primary oral spines, and color. The distinct spoon-shaped valves of the tridentate pedicellariae in *A. cucullatum* sp. nov. are not present in *A. coriaceum*. In addition, in *A. coriaceum*, the rostrate form of the tridentate pedicellariae has a coarsely serrated blade (see Plate LXXIX, Figures 10–15 in Mortensen, 1935). The hoof of the primary oral spines in *A. coriaceum* is smaller than that in *A. cucullatum* sp. nov. The coloration of *A. coriaceum* (greenish black or blackish brown) is quite distinct from that of *A. cucullatum* sp. nov. (light brown) (Agassiz, 1879).

Araeosoma polyporum sp. nov.

Diagnosis

Color of test is translucent, the tubercles and apical system red, oral tube feet and peristome buff, and the membranous gaps and spines white. Membranous spaces widest in the median area between the plates of the column. A primary tubercle occurs on every interambulacral plate on the oral surface, forming a regular adradial series. Some aboral plates have four pore pairs. The hoof of the primary oral spines is white, relatively short (about 0.5 mm), and only slightly flared. Involute tridentate pedicellariae with long, narrow blades, the tip round (Figures 7, 8).

Holotype

MBM286949, a seamount near the Mariana Trench, station FX-Dive 64 (11°18' N, 139°21' E), depth 207 m, June 22, 2016.

Etymology

Named *polyporum*, from the Greek word *poly* (many) and *porus* (pore), after the four pore pairs present in aboral plates.

Description

Test of holotype (Figures 7A, B): Approximately 46.4 mm TD, flexible, flattened, and pentagonal in outline. Color of test is translucent, tubercles and apical system red, oral tube feet and peristome buff, and the membranous gaps and spines white. Ratio of ambulacrum to interambulacrum width at ambitus, 1:2.

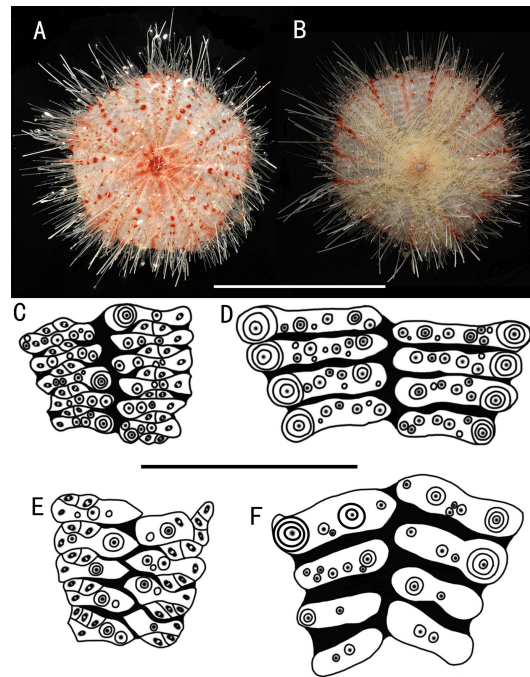


FIGURE 7

Araeosoma polyporum sp. nov.; holotype, MBM286949 (test diameter, 46.4 mm). (A) Aboral view. (B) Oral view. (C–F) Details of the coronal plates: (C), oral ambulacra (D), oral interambulacra (E), aboral ambulacra (F) aboral interambulacra. Scale bars, 50 mm (A, B) and 10 mm (C–F).

There are 41–45 plates in each column of the interambulacra, with about 20–22 of these plates on the oral surface. There are 61–64 plates in each column of the ambulacra, with about 30–32 of these plates on the oral surface. Membranous spaces widest in the median area between the plates of the column. Adapical-most interambulacra plates angled slightly.

Oral test plating (Figures 7C, D): A primary tubercle occurs on every interambulacra plate from the edge of the peristome to the ambitus, forming a regular adradial series. A smaller primary tubercle occurs on a few plates. These tubercles form an irregular series adjacent to the interradius. Numerous secondary and miliary tubercles scattered over these plates. In the ambulacra, a primary tubercle occurs on a few plates, forming an irregular perradial series. Numerous secondary and miliary tubercles are scattered over these plates.

The peristome is approximately 17 mm in diameter, with about 10 boomerang-shaped plates in each column. Each plate has a row of two to three tubercles. The pore pairs are arranged in a single series. Peristomial spines and tube feet buff. Gills small.

Aboral test plating (Figures 7E, F): A primary tubercle occurs on each or every second interambulacra plate from the ambitus to about half of the test, forming an irregular adradial series. One secondary tubercle occurs on a few plates. Numerous miliary tubercles are scattered over these plates. In the ambulacra, a primary tubercle occurs on every plate or every

second or every third plate, forming an irregular perradial series. Numerous secondary and miliary tubercles are scattered over these plates. The pore pairs are arranged into three discrete columns in series, gradually curved near the apical system. Some plates have four pore pairs.

The apical system measures 9 mm in diameter, sub-pentagonal. Genital pores are large, opening in the membranous space at the genital plates. Madreporite distinct, slightly raised, and kidney-shaped. Ocular plates are small, with two to three small tubercles.

Spines: Hollow and cylindrical, with the longest approximately 25 mm long, 0.3 mm in diameter. The primary spines of the oral surface are smooth, slightly curved, and with about 20 fine, longitudinal striations. The hoof of the primary oral spines is white and relatively short (about 0.5 mm) and only slightly flared.

Pedicellariae (Figure 8): Two kinds of tridentate pedicellariae are present. One an involute form (head length about 1.8 mm) with long, narrow, and un-serrated blades, tip rounded, and almost the same width of the base; the valves touch only at the widened tip. The other a rostrate form (about 1.5 mm long) with straight-sided blades and an un-serrated tip only slightly narrowing toward the base. The valves are in contact for most of their length. Triphyllous pedicellariae (about 0.3–0.4 mm) of the typical echinothurioid form. Dactyloous pedicellariae not found.

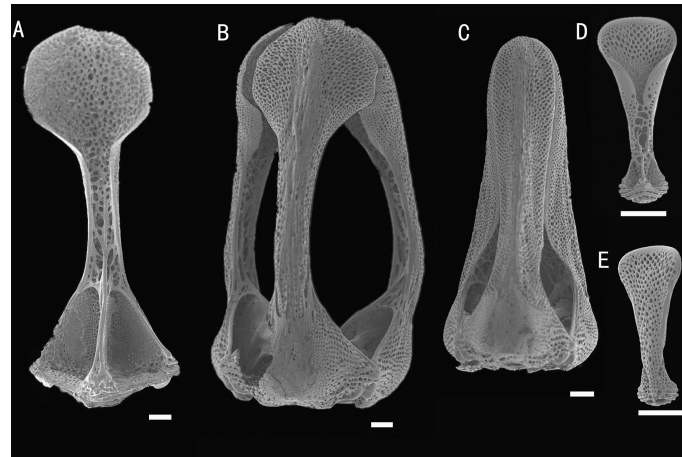


FIGURE 8

Araeosoma polyporum sp. nov.; holotype, MBM286949. SEM images of pedicellariae. (A, B) Involute tridentate pedicellaria: (A) individual valve (B) head. (C) Rostrate tridentate pedicellaria. (D, E) Valves of triphyllous pedicellariae. Scale bar, 100 μ m.

Size range

The TD of the single known specimen is 46.4 mm.

Distribution

Found only on a seamount near the Mariana Trench in the Northwest Pacific Ocean, where the water depth is about 207 m.

Remarks

The pore pairs of *A. polyporum* sp. nov. reach up to four in some aboral plates, making it most similar to *Araeosoma owstoni* Mortensen, 1904 (known from the Western Pacific Ocean). *A. polyporum* sp. nov. differs from *A. owstoni* in terms of the presence of the involute form of tridentate pedicellariae and the hoof of the primary oral spines being relatively shorter than that in *A. owstoni*. The coloration of the holotype of *A. owstoni* (flesh colored, aboral spines greenish) is quite distinct from that of *A. polyporum* sp. nov. (red, spines white). However, the Hawaiian specimens showed a wide range of color (the small individuals are white, medium-sized specimens are reddish or brick red, and the larger specimens are dull pale purplish and the spines pinkish) (Agassiz and Clark, 1909).

Araeosoma alternatum Mortensen, 1934

Araeosoma coriaceum Döderlein, 1906: 122. *Araeosoma alternatum* Mortensen, 1934:165; 1935:270; Anderson, 2013:556–559 (Figures 9, 10).

Material examined

MBM286966, Y3 seamount, station FX-Dive 21 (8°51' N, 137°47' E), depth 307–381 m, December 24, 2014.

Description

Test (MBM286966) (Figures 9A, B): Approximately 135.4 mm TD, flexible, flattened, and pentagonal in outline. Color of ethanol-preserved test and appendages, nude. Ratio of ambulacrum to interambulacrum width at ambitus, 9:10.

There are 81 plates in each column of the interambulacrum, with about 40 of these plates on the oral surface. There are 147 in each column of the ambulacrum, with about 58 of these plates on the oral surface. Membranous spaces widest in the median area between interambulacrum plates on the aboral surface. These gaps are relatively narrow compared with other *Araeosoma* species. Adapical-most interambulacrum plates angled slightly.

Oral test plating (Figures 9C, D): A primary tubercle occurs on every second interambulacrum plate (a few occur on every plate) from the edge of the peristome to the ambitus, forming a regular adradial series. The other primary tubercles occur on every plate or every second plate, forming an irregular interradius series. Numerous secondary and miliary tubercles are scattered over these plates. In the ambulacra, a primary tubercle occurs on every plate or every second or third plate, forming an irregular perradial series. Secondary tubercles are arranged irregularly on the adradial and perradial sides of the pore pairs. Numerous miliary tubercles are scattered over these plates. The peristome is approximately 38 mm in diameter, with about 11 boomerang-shaped plates in each column. Each plate has a row of two to three tubercles. The pore pairs are arranged in a single series. The peristomial spines and tube feet are nude colored, the same color as that of the test. Gills small.

Aboral test plating (Figures 9E, F): A primary tubercle occurs on a few interambulacrum plates from the ambitus to about half of the test, forming an irregular adradial series. The other primary tubercles occur on a few interambulacrum plates from the ambitus to

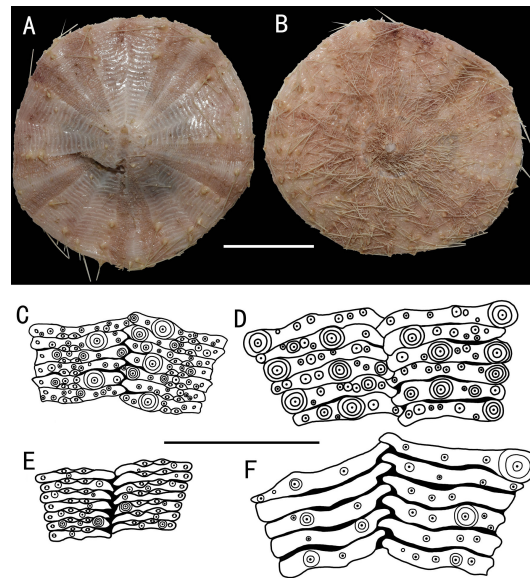


FIGURE 9

Araeosoma alternatum, MBM286966 (test diameter, 135.4 mm). (A) Aboral view. (B) Oral view. (C–F) Details of the coronal plates: (C), oral ambulacra (D), oral interambulacra (E), aboral ambulacra (F) aboral interambulacra. Scale bars, 50 mm (A, B) and 20 mm (C–F).

about half of the test, forming an irregular interradius series. In the ambulacra, a primary tubercle occurs on a few plates, forming an irregular perradial series. There are one to two secondary tubercles in a column of the ambulacra near the apical system. Numerous miliary tubercles are scattered over these plates.

The apical system measures 20 mm in diameter, circle. Genital pores are small, opening in the membranous space at

the genital plates. Madreporite oval, not much raised. The ocular plate is large, with one to three small tubercles.

Spines: Hollow and cylindrical, with the longest approximately 32 mm long, 0.6 mm in diameter. The primary spines of the oral surface are smooth, slightly curved, and with about 20 fine, longitudinal striations. The hoof of the primary oral spines is short and widely flaring (about 0.8 mm).

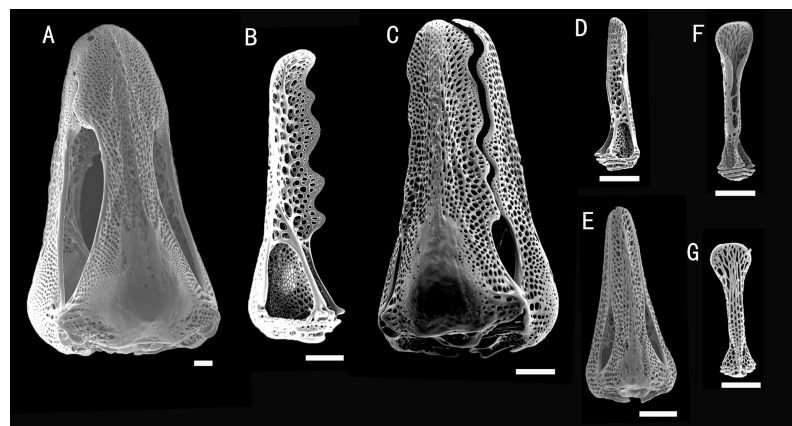


FIGURE 10

Araeosoma alternatum, MBM286966. SEM images of pedicellariae. (A) Large involute tridentate pedicellaria. (B, C) Large rostrate tridentate pedicellaria: (B) individual valve (C) head. (D, E) Small tridentate pedicellaria: (D) individual valve (E) head. (F, G) Valves of triphyllous pedicellariae. Scale bar, 100 μ m.

Pedicellariae (Figure 10): Three kinds of tridentate pedicellariae are present. One is a large (head length about 1.8 mm) involute form, coarsely serrated, and the tip widening to half the width of the base. The valves are in contact for most of the tip length. The other is a large rostrate form (head length about 0.8 mm, base about 0.35 mm wide), with a coarsely serrated blade widening toward the base. The valves are in contact for most of their length. Another is a small tridentate rostrate form (about 0.5 mm long) with straight-sided, narrow, and un-serrated blades. The valves are in contact for most of their length, with a base about two times the width of the tip. Triphyllous pedicellariae (about 0.38 mm long) with a cylindrical middle, the blades involute and particularly elongated, the base about as wide as the tip, on a long neck and stalk. These unusual triphyllous pedicellariae are readily found on the specimens examined. Dactylous pedicellariae not found.

Distribution

Depth of 307–1,289 m, in the western Indian Ocean, New Caledonia, New Zealand, Southeast Australia, and the Yap Trench area in the Northwest Pacific Ocean.

Remarks

The specimen was clearly a new record for the Northwest Pacific Ocean, as the species was previously known only from the western Indian Ocean and the South Pacific Ocean. The rostrate tridentate pedicellariae and triphyllous pedicellariae in the specimen examined look remarkably similar to Döderlein's figures of *A. alternatum* (see Tafel XXXVIII in Döderlein, 1906). We noticed some differences, including: 1) the absence of ophicephalous pedicellariae compared to the Auckland Island specimens (see Figure 31 in Anderson, 2013); however, the ophicephalous forms are quite rare and very small, and they have not been found on the holotype either; 2) the middle section of the involute tridentate pedicellariae in the specimen examined is relatively wider than that in the type specimen.

Araeosoma bidentatum Anderson, 2013

Araeosoma bidentatum Anderson, 2013:523–529 (Figures 11, 12).

Material examined

MBM286957, M8 seamount, station FX-Dive 224 (10°36' N, 140°04' E), depth 1,314 m, June 12, 2019.

Description

Test (MBM286957) (Figures 11A, B): Approximately 61.5 mm TD, flexible, flattened, and pentagonal in outline. The color of the oral test is buff, sucking disks and peristome orange, and aboral test beige. The membranous connective tissue between the plates is white. Ratio of ambulacrum to interambulacrum width at ambitus, 2:3.

There are 48–52 plates in each column of the interambulacral, with about 19–21 of these plates on the oral surface. There are 51–

58 plates in each column of the ambulacral, with about 21–25 of these plates on the oral surface. Membranous spaces widest in the plates of the interambulacral.

Oral test plating (Figures 11C, D): A primary tubercle occurs on every interambulacral plate from the edge of the peristome to the ambitus, forming a regular adradial series. The other primary tubercles occur on every plate from the edge of the peristome to the ambitus, forming a regular interradius series. Numerous secondary and miliary tubercles are scattered over these plates. In the ambulacra, a primary tubercle occurs on every plate to every third plate, forming an irregular perradial series. One secondary tubercle occurs on a few plates. Numerous miliary tubercles are scattered over these plates.

The peristome is approximately 18 mm in diameter, with about eight boomerang-shaped plates in each column. Each plate has a row of tubercles. The pore pairs are arranged in a single series. The peristomial spines are curved, slightly expanded distally. Gills small.

Aboral test plating (Figures 11E, F): A primary tubercle occurs on every second interambulacral plate from the ambitus to about half of the test, forming a regular adradial series. Numerous secondary and miliary tubercles are scattered over these plates. In the ambulacra, a primary tubercle occurs on a few ambulacra plates from the ambitus to about half of the test, forming an irregular perradial series. Numerous miliary tubercles are scattered over these plates.

The apical system measures 12 mm in diameter, circular. Genital pores are large, opening in the membranous space at the genital plates. Madreporite distinct, slightly raised, and subtriangular. The ocular plate is small, with two to five small tubercles.

Spines: Hollow and cylindrical, with the longest approximately 53 mm long, 0.5 mm in diameter. The primary spines of the oral surface are smooth, slightly curved, and with about 24 fine, longitudinal striations. The hoof of the primary oral spines is white and relatively short (about 0.8 mm), only slightly flared. Primary aboral spines invested in a translucent skin sheath.

Pedicellariae (Figure 12): Three kinds of tridentate pedicellariae are present. One large (about 1.8 mm long) involute form with serrated tips in contact for most of the tip length, with the tip about two-thirds of the width of the base. Two bidentate types are also present. One is straight-sided (about 1.1 mm long) with no involute blades, with the base slightly wider than the blade and the tip slightly serrated. The valves are in contact for most of their length. The other is a rostrate form (about 0.3 mm long) with wide un-serrated blades, only slightly narrowing toward the base. The valves are in contact for most of their length. Triphyllous pedicellariae (about 0.3–0.4 mm) is the typical echinothurioid form. Dactylous (about 2.1 mm): form typical of the genus, with six valves, the blade edges finely “crimped.”

Distribution

Depth of 760–1,314 m, in New Zealand, Australia, and the Caroline Ridge area in the Northwest Pacific Ocean.

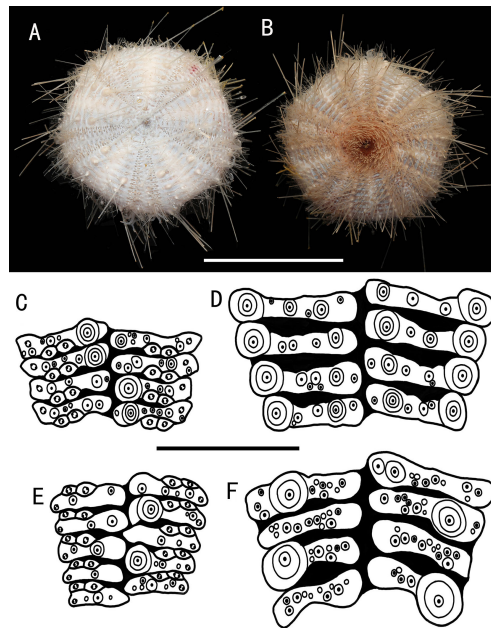


FIGURE 11

Araeosoma bidentatum, MBM286957 (test diameter, 61.5 mm). (A) Aboral view. (B) Oral view. (C–F) Details of the coronal plates: (C), oral ambulacra (D), oral interambulacra (E), aboral ambulacra (F) aboral ambulacra. Scale bars, 50 mm (A, B) and 10 mm (C–F).

Remarks

The specimen was clearly a new record for the Northwest Pacific Ocean, as the species was previously known only from the South Pacific Ocean.

The bidentate pedicellariae are known only from *A. bidentatum*, and this characteristic pedicellaria is common on the single specimen examined. The specimen from the Caroline Ridge area differs from the type specimens regarding the presence of two types of bidentate pedicellariae and the dactyloous pedicellariae with six valves. The type specimens only have one type of bidentate pedicellariae and dactyloous pedicellariae with five valves (see Figure 5 in Anderson, 2013). Additionally, the coloration of the type specimens (deep red) is quite distinct from that of the specimen examined (buff). We believe that these differences are individual differences, and barcoding and the phylogenetic relationships supported this view (see analysis for details; Figure 13).

Barcoding and phylogenetic relationships

In total, 27 new sequences (14 for *COI* and 13 for *16S*) were obtained (Supplementary Table S2) for *A. alternatum*, *A. polyporum* sp. nov., *A. bidentatum*, *A. cucullatum* sp. nov., and *H. involucreum* sp. nov. For *A. cucullatum* sp. nov. and *H. involucreum* sp. nov., multiple specimens (four and seven specimens per species, respectively) were analyzed to document the intraspecific variability. We observed a hierarchical increase in divergence (K2P distance) according to the

different taxonomic levels, within species (from 0% to 0.8%), within congeners (from 1.5% to 12.6%), and within family (16.9%) (Figure 13A). There was a clear barcoding gap for the family Echinothuriidae, which supported the identification of the three new species. The NJ tree showed that the sequencing records for 53 queries representing 12 species formed distinct barcode clusters (Figure 13B), also indicating their successful identification.

In order to explore the phylogenetic position of Echinothuriidae, BI and ML analyses were conducted. The phylogenetic trees resulting from both BI and ML analyses were congruent and generally well supported (Figure 13C). Tree topologies supported the closed relationship of Echinothuriidae and Phormosomatidae. The order Echinothurioida grouped with the lineage Aspidodiadematoidea + Pedinoidea. Within the family Echinothuriidae, different specimens of *A. cucullatum* sp. nov. and *H. involucreum* sp. nov. were grouped together with high support (BP = 99%–100%, PP = 1.00). The monophyly of the genus *Araeosoma* was well supported (BP = 100%, PP = 1.00). The monophyly of *Hygrosoma* could not be verified because only *H. involucreum* sp. nov. was included in our study; however, it was supported to be a sister to *Araeosoma* (BP = 99%, PP = 1.00).

Biogeographic analyses

The UPGMA cluster analysis found 10 main groups among the 29 deep-sea fields (Figure 14): East Pacific Rise and Northern Atlantic Boreal (1–3), Yap Trench and Indian Ocean (4–5),

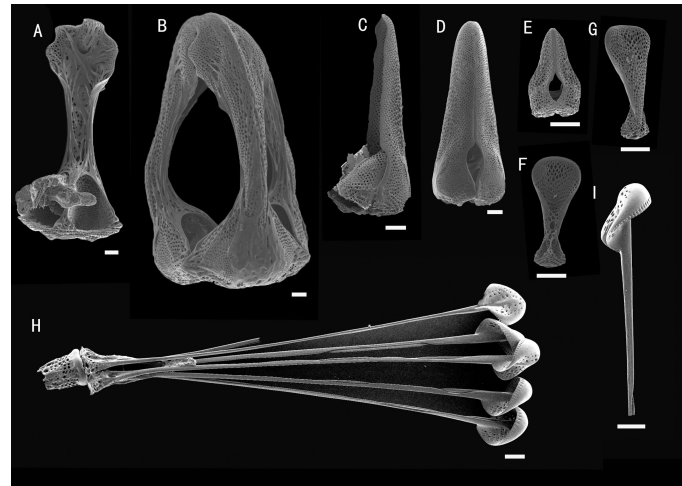


FIGURE 12

Araeosoma bidentatum, MBM286957. SEM images of pedicellariae. (A, B) Large tridentate pedicellaria: (A) individual valve (B) head. (C, D) Straight side bidentate pedicellaria: (C) individual valve (D) head. (E) Rostrate bidentate pedicellaria. (F, G) Valves of triphylous pedicellariae. (H, I) Dactylose pedicellaria. Scale bar, 100 μm .

Western and Central Pacific (6–7), Northern Pacific Boreal (8), North Indian Ocean (9–10), Southwest Pacific (11–13), Indo-Pacific (14–18), Atlantic (19–24), Mariana Trench (25), and Caroline Ridge and the Magellan seamount (26–29). The Mariana Trough, Yap Trench, and Caroline Ridge formed separated groups from each other. The Kocebu Guyot of the Magellan seamount clustered together with Caroline Ridge M4, M5, and M7. However, only one shared species was found in these seamounts, suggesting the low connectivity between seamount populations.

Discussion

Diversity and distribution of echinothuriids

Echinothuriids comprise an abundant echinoderm group widely distributed in deep water. Among the echinothuriid genera inhabiting deep water, *Araeosoma* Mortensen, 1903 was observed in the highest abundance, with a total of 21 valid species including the four newly described species here (Figure 15). To date, 20 species of *Araeosoma* have been discovered in Pacific Ocean deep water, except for *Araeosoma belli* Mortensen, 1903, which was reported from the Gulf of Mexico and the Caribbean Sea (Felder and Camp, 2009; Alvarado, 2010). Among these 20 species, 18 occurred in the Western Pacific. Compared to the abundance of *Araeosoma*, only nine species of *Sperosoma* Koehler, 1897, seven species of *Tromikosoma* Mortensen, 1903, four species of *Hygrosoma* Mortensen, 1903, three species of *Hapalosoma* Mortensen, 1903, and two species of *Calveriosoma* Mortensen, 1934, have been

described to date (Figure 14). Like *Araeosoma*, the members of *Sperosoma* and *Calveriosoma* are mainly found in the Western Pacific, which hosts about 55.6% and 50.0% of their total numbers, respectively. All members of *Hygrosoma* and *Hapalosoma* are distributed in the Western Pacific, while the members of *Hygrosoma*, *Sperosoma*, and *Calveriosoma* are recorded in the North Atlantic. The members of *Tromikosoma* are likely to be rarer in the West Pacific than in the East Pacific and North Atlantic.

Biogeography of deep-sea echinothuriids

Based on the water temperature, dissolved oxygen, the particulate organic flux to the seafloor, and salinity, Watling et al. (2013) delineated 14 deep-sea benthic provinces in the world ocean: Arctic Bathyal, North Pacific Boreal, West Pacific Bathyal, Southeast Pacific Ridges, North Pacific Bathyal, Antarctic Bathyal, North Atlantic Boreal, North Atlantic Bathyal, Cocos Plate, Subantarctic, Nazca Plate, New Zealand Kermadec, Indian Ocean Bathyal, and South Atlantic. This model needs to be examined with documented locations of select benthic marine species.

Based on the distribution data of *Araeosoma*, *Sperosoma*, *Tromikosoma*, *Hygrosoma*, *Hapalosoma*, and *Calveriosoma* in deep water, we delineated 10 isolated deep-sea provinces: East Pacific Rise and Northern Atlantic Boreal, Yap Trench and Indian Ocean, Western and Central Pacific, Northern Pacific Boreal, North Indian Ocean, Southwest Pacific, Indo-Pacific, Atlantic, Mariana Trench, and Caroline Ridge and the Magellan seamount (Figure 14). In our analysis, the North and South Indian Oceans likely represent two independent deep-sea

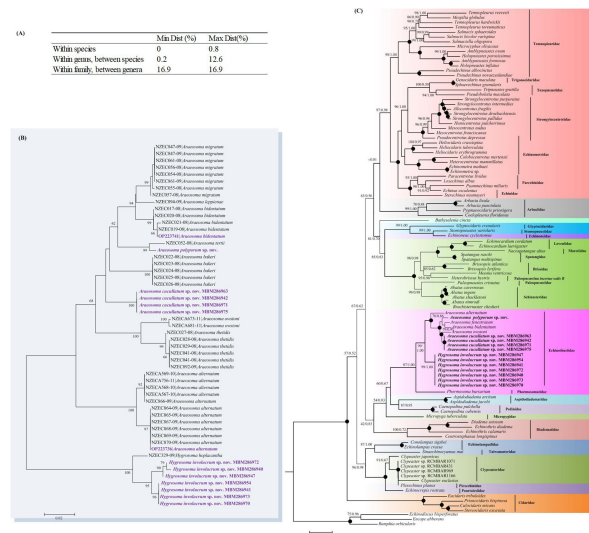


FIGURE 13

(A) *Cytochrome oxidase subunit I (COI)* genetic divergence within echinothuriid species. (B) Neighbor-joining (NJ) tree inferred from the COI sequences showing the relationships of the echinothuriid species based on the Kimura two-parameter (K2P) model. (C) Maximum likelihood (ML) and Bayesian inference (BI) trees of Echinoidea based on the combined sequences of COI and 16S. Numbers at the nodes represent the ML (left) and BI (right) support values. Only values higher than 0.50 are shown. Newly sequenced echinothuriids are in bold.

provinces, while the East Pacific Rise and Northern Atlantic Boreal appear to represent a combined province rather than independent ones, which did not coincide with the model provided by Watling et al. (2013). In the present study, the Western Pacific likely included six provinces. Similar to the models proposed in previous studies (Bachraty et al., 2009;

Rogers et al., 2012; Watling et al., 2013; Wu et al., 2019), the Western Pacific was geographically more complex than initially thought. In the study of Bachraty et al. (2009), the Western Pacific represented two provinces. Similarly, the Western Pacific was regarded as three provinces in Watling et al. (2013) and Wu et al. (2019) and four provinces in Rogers et al. (2012). Previous

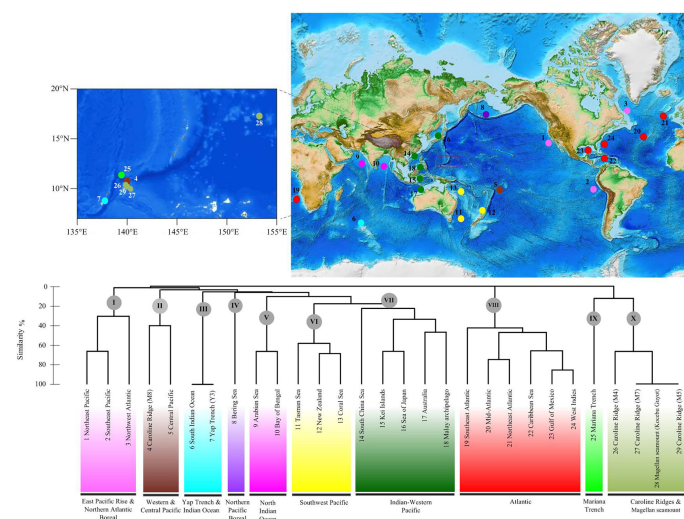


FIGURE 14

Geographical clustering of the 29 deep-sea fields studied based on the unweighted pair group method with arithmetic mean (UPGMA) cluster analysis (Bray–Curtis distance) and an 10-province model based on the data of deep-sea echinothuriid species.

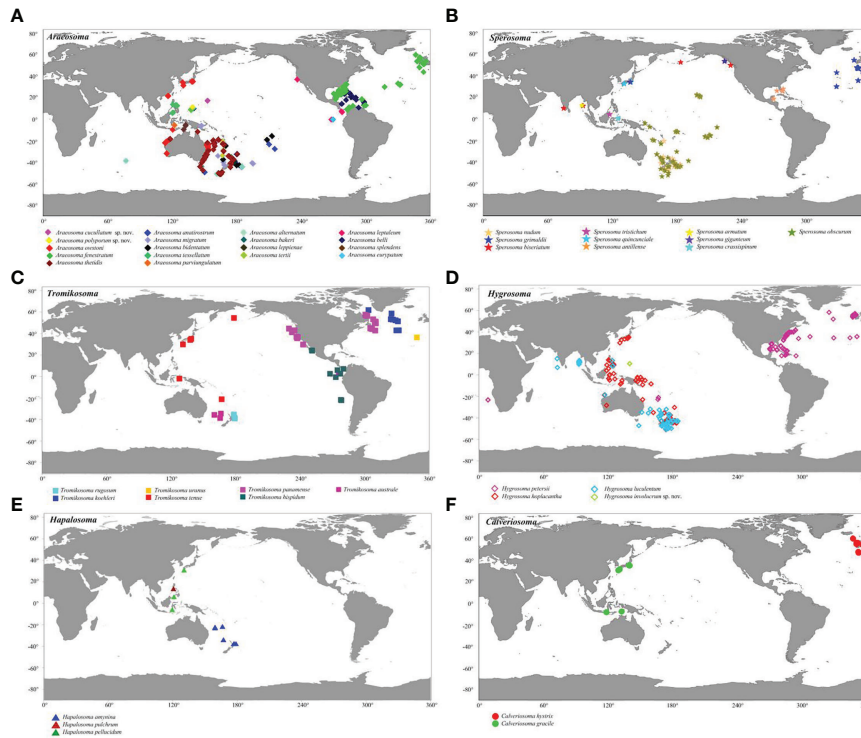


FIGURE 15
 Distribution of deep-sea echinothuriid species based on the records of the Ocean Biodiversity Information System (<https://obis.org/>).
 (A) *Araeosoma* Mortensen, 1903. (B) *Sperosoma* Koehler, 1897. (C) *Tromikosoma* Mortensen, 1903. (D) *Hygrosoma* Mortensen, 1903.
 (E) *Hapalosoma* Mortensen, 1903. (F) *Calveriosoma* Mortensen, 1934. Colors denote different echinothuriid species.

studies have proposed the East Pacific Rise as the biogeographic center of deep-sea hydrothermal vent fauna (Van Dover and Hessler, 1990; Bachraty et al., 2009). The distribution of echinothuriids showed that the Western Pacific harbored the highest species diversity. This result supported the “possible ancestral position of the Western Pacific” (Moalic et al., 2012; Sun et al., 2018).

The Mariana Trough, Yap Trench, and Caroline Ridge formed separated clusters, although their positions are in close proximity. This is consistent with the estimated low connectivity between the seamount populations (de Forges et al., 2000). However, the Kocebu Guyot of the Magellan seamount, which was far away from Caroline Ridge, clustered together with M4, M5, and M7. The Mariana Trough, as an independent province, is in accordance with the partition scheme of the Northwest Pacific suggested by Kojima and Watanabe (2015) and Wu et al. (2019). Due to the lack of data regarding echinothuriids from these seamounts, we were unable to further delineate the deep-sea provinces, especially those in the Magellan seamount and Caroline Ridge. The 10-province model still needs to be examined by complementary data on other seamounts and other animals.

Conclusion

Based on the examination of specimens of Echinothuriidae collected from seamount areas [Magellan (Kocebu Guyot), Yap (Y3), and Mariana and Caroline (M4, M5, M7, and M8)] in the Northwest Pacific Ocean from 2014 to 2019, we identified three new species—*Araeosoma cucullatum* sp. nov., *Araeosoma polyporum* sp. nov., and *Hygrosoma involucrum* sp. nov.—and two new records including two species from the genus *Araeosoma*. The characteristics of the coloring, ambulacrum, interambulacrum, apical system, spines, and pedicellariae of these species were different from each other and their congeners. There was a clear barcoding gap (K2P genetic distance) for the family Echinothuriidae, and the NJ tree showed distinct barcode clusters for these species, which supported the identification of the five new species. The BI and ML analyses revealed the monophyly of Echinothuriidae. Moreover, UPGMA cluster analysis revealed 10 deep-sea provinces: East Pacific Rise and Northern Atlantic Boreal, Yap Trench and Indian Ocean, Western and Central Pacific, Northern Pacific Boreal, North Indian Ocean, Southwest Pacific, Indo-Pacific, Atlantic, Mariana Trench, and Caroline Ridge and Magellan seamount. Our analysis revealed low connectivity between

the seamount populations. The Western Pacific is geographically complex and harbors a higher species diversity of deep-sea echinothuriids than other sea areas, suggesting the pivotal role of the Western Pacific in the dispersal and speciation of deep-sea echinothuriids.

Data availability statement

The datasets presented in this study can be found in online repositories. The names of the repository/repositories and accession number(s) can be found in the article/[Supplementary Material](#).

Author contributions

WZ, SS, ZS, and NX conceived and designed the research. WZ and NX studied the morphology. SS performed the barcoding, phylogenetic relationship, and biogeographic analyses. WZ, SS, ZS, and NX contributed to the writing and editing of the final manuscript. All authors contributed to the article and approved the submitted version.

Funding

This work was supported by the Strategic Priority Research Program of the Chinese Academy of Sciences (XDA22050302 and XDB42000000), the Key Program of National Natural Science Foundation of China (no. 41930533), the National Key Research and Development Program of China (2021YFE0193700), and the National Science Foundation for Distinguished Young Scholars (42025603).

Acknowledgments

We thank the assistance of the crew of R/V *KEXUE* and ROV *FaXian* for sample collection and Dr. Kunxuan Li for photographing freshly collected specimens. We also appreciate

References

- Agassiz, A. (1879). "Preliminary report of the echini of the exploring expedition of H.M.S. challenger," *American Academy of Arts And Sciences in Proceedings of the American Academy of Arts and Sciences. new series*, (Cambridge: American Academy of Arts & Sciences) 6. 190–212. doi: 10.2307/25138537
- Agassiz, A. (1880). Reports of the dredging by the *Blake*-Preliminary report on the echini. *Bull. Museum. Comp. Zool. Harvard*. 8, 69–84.
- Agassiz, A., and Clark, H. L. (1909). Hawaiian And other pacific echini. the echinothuridae. *Memoirs. Museum. Comp. Zool.* 34 (3), 192.
- Alvarado, J. J. (2010). Echinoderm diversity in the Caribbean Sea. *Mar. Biodivers.* 41 (2), 261–285. doi: 10.1007/s12526-010-0053-0

the reviewers for their constructive comments on an earlier version of the manuscript.

Conflict of interest

The authors declare that the research was conducted in the absence of any commercial or financial relationships that could be construed as a potential conflict of interest.

Publisher's note

All claims expressed in this article are solely those of the authors and do not necessarily represent those of their affiliated organizations, or those of the publisher, the editors and the reviewers. Any product that may be evaluated in this article, or claim that may be made by its manufacturer, is not guaranteed or endorsed by the publisher.

Supplementary material

The Supplementary Material for this article can be found online at: <https://www.frontiersin.org/articles/10.3389/fmars.2022.1036914/full#supplementary-material>

SUPPLEMENTARY TABLE 1

The primer sequences for COI and 16S genes.

SUPPLEMENTARY TABLE 2

The Echinoidea species used in the barcoding and phylogenetic analyses.

SUPPLEMENTARY TABLE 3

The best-fit partitioning schemes and substitution models.

SUPPLEMENTARY TABLE 4

The distribution data of echinothuriid species.

SUPPLEMENTARY TABLE 5

Raw presence-absence (0-1) data for echinothuriid species used in the statistical analyses.

- Anderson, O. F. (2013). A review of new zealand and southeast australian echinothuriinids (echinodermata: echinothuriidae) with descriptions of seven new species. *Zootaxa* 3609 (6), 521. doi: 10.11646/zootaxa.3609.6.1

- Anderson, O. F. (2016). A review of new zealand and southeast australian echinothurioids (echinodermata: echinothurioida)—excluding the subfamily echinothuriinae—with a description of a new species of tromikosoma. *Zootaxa* 4092 (4), 451. doi: 10.11646/zootaxa.4092.4.1

- Bachraty, C., Legendre, P., and Desbruyeres, D. (2009). Biogeographical relationships among deep-sea hydrothermal vent faunas at global scale. *Deep-Sea. Res. I.* 56, 1371–1378. doi: 10.1016/j.dsr.2009.01.009

- Claus, C. F. W. (1880). *Grundzuge der zoologie. 4th Edition* Vol. 821 (Marburg and Leipzig: N. G. Elwertsche Universitätsbuchhandlung), 522 pp.

- Coppard, S. E., and Schultz, H. A. G. (2006). A new species of coelopleurus (Echinodermata: Echinoidea: Arbaciidae) from new Caledonia. *Zootaxa* 1281, 1–19. doi: 10.11646/zootaxa.1281.1.1
- David, B., and Sibuet, M. (1985). “Distribution et diversité des échinides,” in *Peuplements profonds du golfe de gascogne*. Eds. L. Laubier and C. Monniot (France: IFREMER), 509534.
- de Forges, B. R., Koslow, J. A., and Poore, G. C. B. (2000). Diversity and endemism of the benthic seamount fauna in the southwest pacific. *Nature* 405, 944–947. doi: 10.1038/35016066
- Döderlein, L. (1906). “Die echinoiden der deutschen tiefsee-expedition,” in *Wissenschaftliche ergebnisse der deutschen tiefsee-expedition auf dem dampfer “Valdivia” 1898–1899*, (Jena: VERLAG VON GUSTAV FISCHER) 5, 61–290.
- Felder, D. L., and Camp, D. K. (Eds.) (2009). *Gulf of Mexico: origin, waters, and biota. volume 1, biodiversity* (Bizzell St, College Station; Texas A&M University Press) 1393 pp.
- Grube, A. E. (1868). *Asthenosoma varium*. *Jahresbericht. und. Abhandlungen. der. Schlesischen. Gesellschaft. für. Vaterländische. Cultur.* 45 (1867), 42–44.
- Hoareau, T. B., and Boissin, E. (2010). Design of phylum-specific hybrid primers for dna barcoding: addressing the need for efficient coi amplification in the echinodermata. *Mol. Ecol. Resour.* 10 (6), 960–967. doi: 10.1111/j.1755-0998.2010.02848.x
- Jeffery, C. H., Emlet, R. B., and Littlewood, D. (2003). Phylogeny and evolution of developmental mode in temnopleurid echinoids. *Mol. Phylogenet. Evol.* 28 (1), 99–118. doi: 10.1016/S1055-7903(03)00030-7
- Katoh, K., Kuma, K., Toh, H., and Miyata, T. (2005). MAFFT version 5: improvement in accuracy of multiple sequence alignment. *Nucleic Acids Res.* 33, 511518. doi: 10.1093/nar/gki198
- Koehler, R. (1897). Nouveau genre d’Echinothuride. *Zoologischer. Anzeiger.* 20, 302–307.
- Kojima, S., and Watanabe, H. (2015). *Vent fauna in the Mariana Trough*. In: *Subseafloor Biosphere Linked to Hydrothermal Systems: TAIGA Concept*. Eds. J.-i. Ishibashi, K. Okino and M. Sunamura Springer, Tokyo, Japan, pp. 313–323.
- Kroh, A., and Mooi, R. (2022). World echinoidea database. *Sperosoma*. Accessed through: World Register of Marine Species Available at: <https://www.marinespecies.org/aphia.php?p=taxdetails&id=123402>.
- Lanfear, R., Frandsen, P. B., Wright, A. M., Senfeld, T., and Calcott, B. (2016). Partitionfinder 2: new methods for selecting partitioned models of evolution for molecular and morphological phylogenetic analyses. *Mol. Biol. Evol.* 34, 772773. doi: 10.1093/molbev/msw260
- Minh, B. Q., Nguyen, M. A. T., and von Haeseler, A. (2013). Ultrafast approximation for phylogenetic bootstrap. *Mol. Biol. Evol.* 30, 1188–1195. doi: 10.1093/molbev/mst024
- Moalic, Y., Desbruyeres, D., Duarte, C. M., Rozenfeld, A. F., Bachraty, C., and Arnaud-Haond, S. (2012). Biogeography revisited with network theory: retracing the history of hydrothermal vent communities. *Syst. Biol.* 61, 127137. doi: 10.1093/sysbio/syr088
- Mooi, R., Constable, H., Lockhart, S., and Pearse, J. (2004). Echinothurioid phylogeny and the phylogenetic significance of *Kamptosoma* (Echinoidea: Echinodermata). *Deep. Sea. Res. Part II.* 51 (14/16), 1903–1919. doi: 10.1016/j.dsr2.2004.07.020
- Mortensen, T. (1903). Echinoidea (Part i). *Danish. Ingolf-Expedition.* 4 (1), 1–198.
- Mortensen, T. (1904). On some echinothurids from Japan and the Indian ocean. *Ann. Magazine. Natural History. Seventh. Ser.* (Oxford University Press) 14, 81–93. doi: 10.1080/03745480409442975
- Mortensen, T. (1927). *Handbook of the echinoderms of the British isles* (Oxford, UK: Oxford University Press), 471 pp.
- Mortensen, T. (1934). New echinoidea. preliminary notice. *Videnskabelige. Meddelelser. Dansk. Naturhistorisk. Forening. i. København.* 98, 161–167.
- Mortensen, T. (1935). *A monograph of the echinoidea II. bothriocidaroida, melonechinoidea, lepidocentroida and stirodonta*. Ed. C. A. Reitzel (Copenhagen: Oxford University Press) 647 pp.
- Rambaut, A., Drummond, A. J., Xie, D., Baele, G., and Suchard, M. A. (2018). Posterior summarization in bayesian phylogenetics using tracer 1.7. *Syst. Biol.* 67, 901904. doi: 10.1093/sysbio/syy032
- Rogers, A. D., Tyler, P. A., Connelly, D. P., Copley, J. T., James, R., Larter, T. D., et al. (2012). The discovery of new deep-sea hydrothermal vent communities in the southern ocean and implications for biogeography. *PLoS Biol.* 10 (1), e1001234. doi: 10.1371/journal.pbio.1001234
- Ronquist, F., and Huelsenbeck, J. P. (2003). MrBayes 3: Bayesian phylogenetic inference under mixed models. *Bioinformatics* 19, 1572–1574. doi: 10.1093/bioinformatics/btg180
- Smith, A. B., and Wright, C. W. (1990). British Cretaceous Echinoids. part 2, echinothurioida, diadematoidea, and stirodonta (1, calycina). *Monograph. Palaeontol. Soc.* 143, 101–198. doi: 10.1080/25761900.2022.12131767
- Stevenson, A., and Kroh, A. (2020). “Deep-sea sea urchins,” in *Sea Urchins: Biology and ecology* (Amsterdam: Elsevier). *fourth edition*, vol. 43. doi: 10.1016/B978-0-12-819570-3.00014-7
- Sun, S., Sha, Z. L., and Wang, Y. R. (2018). Phylogenetic position of alvinocarididae (Crustacea: Decapoda: Caridea): new insights into the origin and evolutionary history of the hydrothermal vent alvinocarid shrimps. *Deep. Sea. Res. Oceanogr. Res. Pap.* 141, 93105. doi: 10.1016/j.dsr.2018.10.001
- Tamura, K., Stecher, G., Peterson, D., Filipowski, A., and Kumar, S. (2013). MEGA6: molecular evolutionary genetics analysis version 6.0. *Mol. Biol. Evol.* 30, 2725–2729. doi: 10.1093/molbev/mst197
- Thomson, C. W. (1872a). Notice of a new family of the Echinodermata. *Proc. R. Soc. Edinburgh.* 7, 615–617. doi: 10.1017/S0370164600042759
- Thomson, W. (1872b). On the echinoidea of the ‘Porcupine’ deep-sea dredging-expeditions. *Proc. R. Soc. London.* 20, 491–497. doi: 10.1098/rspl.1871.0095
- Thomson, W. (1877). “The voyage of the ‘Challenger’: the Atlantic: a preliminary account of the general results of the exploring voyage of H.M.S. in ‘Challenger’ during the year 1873 and the early part of the year 1876 (New York: Harper), 148–149.
- Trifinopoulos, J., Nguyen, L. T., Von Haeseler, A., and Minh, B. Q. (2016). W-IQ-TREE: a fast online phylogenetic tool for maximum likelihood analysis. *Nucleic Acids Res.* 44, W232–W235. doi: 10.1093/nar/gkw256
- Van Dover, C. L., and Hessler, R. R. (1990). “Spatial variation in faunal composition of hydrothermal vent communities on the East pacific rise and Galapagos rift,” in *Gorda ridge: A seafloor spreading center in the united states exclusive economic zone* (New-York: Springer-Verlag).
- Watling, L., Guinotte, J., Clark, M. R., and Smith, C. R. (2013). A proposed biogeography of the deep ocean floor. *Prog. Oceanogr.* 111 (apr.), 91–112. doi: 10.1016/j.pocan.2012.11.003
- Wu, X., Zhan, Z., and Xu, K. (2019). Two new and two rarely known species of branchinotoglua (annelida: polynoidae) from deep-sea hydrothermal vents of the manus back-arc basin, with remarks on the diversity and biogeography of vent polynoids. *Deep-Sea. Res.* (JUL.) 149. doi: 10.1016/j.dsr.2019.05.011